

Thermal-expansion behavior of a directionally solidified NiAl–Mo composite investigated by neutron diffraction and dilatometry

H. Bei^{a)} and E. P. George^{b)}

Department of Materials Science and Engineering, The University of Tennessee, Knoxville, Tennessee 37996 and Metals and Ceramics Division, Oak Ridge National Laboratory, Oak Ridge, Tennessee 37831

D. W. Brown

Lujan Center, Los Alamos National Laboratory, Los Alamos, New Mexico 87545

G. M. Pharr and H. Choo

Department of Materials Science and Engineering, The University of Tennessee, Knoxville, Tennessee 37996 and Metals and Ceramics Division, Oak Ridge National Laboratory, Oak Ridge, Tennessee 37831

W. D. Porter

Metals and Ceramics Division, Oak Ridge National Laboratory, Oak Ridge, Tennessee 37831

M. A. M. Bourke

Lujan Center, Los Alamos National Laboratory, Los Alamos, New Mexico 87545

(Received 21 January 2005; accepted 15 April 2005; published online 16 June 2005)

The thermal expansion of directionally solidified NiAl–Mo eutectic alloys consisting of nanoscale Mo fibers embedded in a NiAl matrix was analyzed by neutron diffraction and dilatometry. From room temperature to 800 °C, perpendicular to the fiber direction, the NiAl and Mo phases expand independently with average coefficients of thermal expansion (CTEs) of $16.0 \times 10^{-6} \text{ °C}^{-1}$ and $5.8 \times 10^{-6} \text{ °C}^{-1}$, respectively. Parallel to the fiber direction, they coexpand up to 650 °C with an average CTE of $12.8 \times 10^{-6} \text{ °C}^{-1}$, but above this temperature the Mo fibers expand more than the NiAl matrix. This anomalous behavior is the result of the load transfer to the Mo fibers when the NiAl matrix softens. The average CTE of the composite parallel to the fiber direction was determined by dilatometry to be $13.0 \times 10^{-6} \text{ °C}^{-1}$, which is approximately 11% lower than the value predicted by a simple rule of mixtures using the CTEs of the constituent phases. © 2005 American Institute of Physics. [DOI: 10.1063/1.1929853]

INTRODUCTION

NiAl-based composites have been investigated as potential high-temperature structural materials.^{1–5} An example is the NiAl–Mo eutectic which, when solidified from the melt, forms an *in situ* composite consisting of Mo_{ss} (solid-solution) fibers embedded in a NiAl matrix.^{6–10} By carefully controlling the solidification conditions, the fibers can be grown quite long (practically continuous, with aspect ratios > 250).¹⁰ Perpendicular to the growth direction, they arrange themselves in a hexagonal pattern.¹⁰ The cross-sectional shape of the Mo fibers is square, with average edge lengths of 400–800 nm and interfiber spacings of 1–2 μm, both of which depend inversely on the square root of the growth rate between 20 and 80 mm/h.¹⁰

In order to understand and model the thermomechanical response of such a composite, it is important to measure the individual thermal and mechanical properties of the constituent phases as well as those of the overall composite.¹¹ For example, the coefficient of thermal expansion (CTE) of a composite determines its overall length change upon heating or cooling, whereas the CTEs of its constituent phases deter-

mine (in part) how much thermally induced internal stresses are generated. Likewise, a stiffness mismatch between the constituent phases may result in mechanically induced internal stresses during loading. These thermal and mechanical stresses are of interest because they can have deleterious effects, including interface debonding, cracking, and elastic/plastic deformation of the constituent phases.

The macroscopic thermal and mechanical properties of composites are typically measured by bulk techniques, such as dilatometry and mechanical testing. In principle, the properties of the constituents can also be deduced from macroscopic measurements, provided bulk materials with the same compositions and structures as those found in the composite are available. However, it is not always possible to produce the individual constituents in monolithic form. In such cases, an *in situ* technique like neutron diffraction can measure phase-specific CTEs.¹² It can also be utilized to study the response of the constituent phases to mechanical loading,^{13,14} that is, the elastic-plastic behavior of the individual phases and load sharing between the phases.

In this study, the phase-specific response of a NiAl–Mo eutectic alloy to thermal and mechanical loading was investigated by neutron diffraction, and the composite response was determined by dilatometry and extensometry.

^{a)}Electronic mail: bei@ornl.gov

^{b)}Author to whom correspondence should be addressed; electronic mail: georgeep@ornl.gov

EXPERIMENTAL PROCEDURES

In situ composites consisting of Mo_{ss} fibers embedded in a NiAl matrix were produced by arc-melting and drop-casting an alloy of composition Ni-45.5Al-9Mo (at. %), followed by directional solidification in a high-temperature optical floating-zone furnace. All compositions in this paper are given in at. %, unless otherwise noted. Details of the processing and its effects on microstructure have been described elsewhere.¹⁰ Button-head tensile specimens with a gage length of 50.80 mm and gage diameter of 5.08 mm were machined from these composites, with the tensile direction parallel to the fiber direction (which is also the solidification direction of the composites).

The phase-specific response of the composite to thermal and mechanical loading was studied by time-of-flight neutron diffraction on the Spectrometer for Materials Research at Temperature and Stress (SMARTS) at the Los Alamos Neutron Science Center (LANSCE) at the Los Alamos National Laboratory.¹⁵ To facilitate simultaneous heating and loading, the sample was held in the SMARTS furnace-load frame combination which is described in detail elsewhere.¹⁵ Briefly, the sample was held at a constant 20 MPa tensile stress at 45° to the incident beam, while diffraction patterns were recorded in detector banks at $\pm 90^\circ$ from the incident beam at temperatures between room temperature and 800°C . In this geometry, diffraction patterns are collected with the scattering vectors parallel to the axial (i.e., fiber) and transverse directions simultaneously. Subsequently, diffraction data were recorded at incrementally higher levels of applied tensile stress until sample failure. The sample was aligned such that the $\{00l\}$ diffraction peaks of the NiAl and Mo_{ss} phases appeared in the center tube of both the axial and transverse detector banks. The d spacings for the individual reflections from NiAl ($B2$ structure) and Mo_{ss} (bcc structure) were determined from single-peak fitting of the (200) peak in both phases using the RAWPLOT utility of the GENERAL STRUCTURE ANALYSIS SOFTWARE (GSAS).¹⁶ The elastic lattice strain in a specific phase, ε , was calculated from

$$\varepsilon = \frac{d_i - d_0}{d_0}, \quad (1)$$

where d_i is the d spacing of a given crystal plane measured during heating and/or loading and d_0 is the corresponding d spacing at room temperature (25°C) and 20 MPa load. In the dilatometer experiments, the thermal strain of the overall composite was obtained by measurements of the actual length of the specimen, that is,

$$\varepsilon^T = \frac{l_T - l_0}{l_0}, \quad (2)$$

where l_T and l_0 are the specimen lengths at elevated and room temperature, respectively.

RESULTS

Microstructure

Figure 1 shows the microstructure of the NiAl–Mo specimens used in this study. The specimens were cut from a

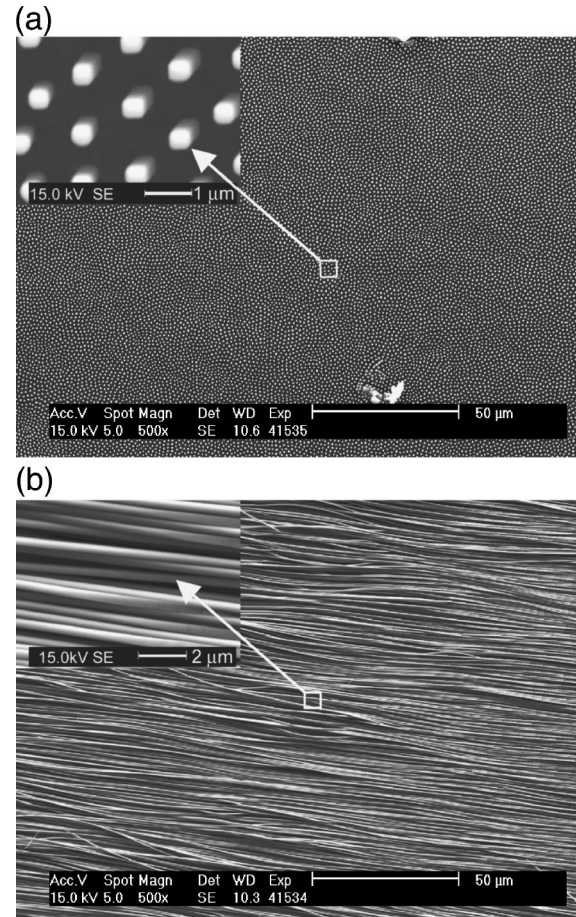


FIG. 1. SEM micrographs showing well-aligned rodlike microstructure of the NiAl–Mo eutectic alloy directionally solidified at 80 mm/h and 60 rpm, with the NiAl matrix preferentially etched: (a) transverse section, (b) longitudinal section.

crystal that was directionally solidified at 80 mm/h and 60 rpm. As discussed in an earlier paper,¹⁰ the microstructure consists of long, single-orientation Mo_{ss} fibers embedded in a single-crystal NiAl matrix, with the growth direction of both phases parallel to the $\langle 100 \rangle$ direction. As shown in the inset in Fig. 1(a), the cross-sectional shape of the Mo_{ss} fibers is square rather than circular. The fibers are ~ 350 nm across, spaced $\sim 1.1 \mu\text{m}$ apart, and have a volume fraction of $\sim 14.1\%$. Electron backscatter diffraction revealed that the NiAl– Mo_{ss} interface boundaries are parallel to the $\{011\}$ planes in both the fiber and the matrix. X-ray microprobe analysis showed that the NiAl matrix contained essentially no Mo ($< 0.1\%$) and had the off-stoichiometric composition Ni-45.2Al, whereas the Mo fibers were a solid solution of all three elements and had the composition Mo-10.1Al-3.9Ni.

Response of the NiAl–Mo composite to thermal loading

Figure 2 shows the $\{200\}$ -specific thermal strains in the NiAl and Mo_{ss} phases of the composite along the transverse direction (i.e., perpendicular to the fiber axis) as a function of temperature. The two phases in the composite expand independently over the entire range of temperature. A similar behavior is also observed in a Ti-6Al-4V matrix composite containing polycrystalline SiC fibers.¹⁷ The average CTEs

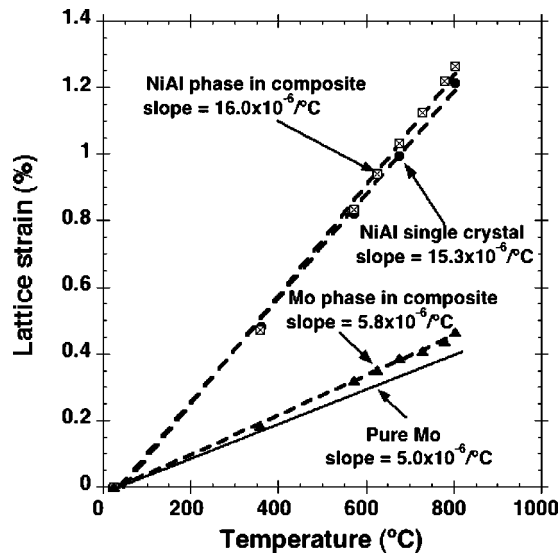


FIG. 2. Temperature dependence of the {200}-specific thermal elastic strain in the NiAl and Mo phases of the composite in the transverse direction. For comparison, the corresponding strains in a NiAl single crystal having the same composition as the NiAl phase in the composite, and in pure Mo, are also shown.

were determined from the slopes of linear fits to the data in Fig. 2 and found to be $16.0 \times 10^{-6} \text{ }^\circ\text{C}^{-1}$ for the NiAl phase and $5.8 \times 10^{-6} \text{ }^\circ\text{C}^{-1}$ for the Mo_{ss} phase.

For comparison, a NiAl single crystal, with composition similar to that of the NiAl matrix in the composite, was grown and its CTE measured. X-ray microprobe analyses showed that the composition of the NiAl single crystal was Ni-47.3Al, which is within 5% of the composition of the NiAl matrix, Ni-45.2Al. This small difference in composition is not expected to affect the thermal-expansion behavior of NiAl as shown previously by Clark and Whittenberger,¹⁸ who investigated alloys having Al contents in the range of 44%–53%. As shown in Fig. 2, the CTE of the monolithic NiAl phase in the {200} direction was found to be $15.3 \times 10^{-6} \text{ }^\circ\text{C}^{-1}$, which is within 5% of that of the NiAl matrix in the composite ($16.0 \times 10^{-6} \text{ }^\circ\text{C}^{-1}$, Fig. 2).

In contrast, the CTE of the Mo_{ss} phase is $5.8 \times 10^{-6} \text{ }^\circ\text{C}^{-1}$, which is 20% greater than that of pure Mo ($5.0 \times 10^{-6} \text{ }^\circ\text{C}^{-1}$),¹² probably because the Mo phase in the composite contains Al ($\sim 10\%$) and Ni ($\sim 4\%$).¹⁰ These elements have lower melting points (660 and 1453 $^\circ\text{C}$, respectively) than does Mo (2610 $^\circ\text{C}$)¹⁹ and, consequently, higher CTEs, $23.1 \times 10^{-6} \text{ }^\circ\text{C}^{-1}$ and $13.4 \times 10^{-6} \text{ }^\circ\text{C}^{-1}$, respectively.¹² They would, therefore, be expected to increase the CTE of Mo when present as alloying elements. To verify this we attempted to arc-melt an alloy having the same composition as the Mo_{ss} fibers and independently determine its CTE. However, we were unsuccessful in making such an alloy because the boiling temperature of Al is lower than the melting point of the Mo, resulting in an almost complete loss of Al during melting.

We next discuss the elastic thermal strain along the axial direction (i.e., parallel to the fiber direction). Figure 3 shows a plot of the temperature dependence of the axial {200}-specific strains in the NiAl and Mo_{ss} phases within the com-

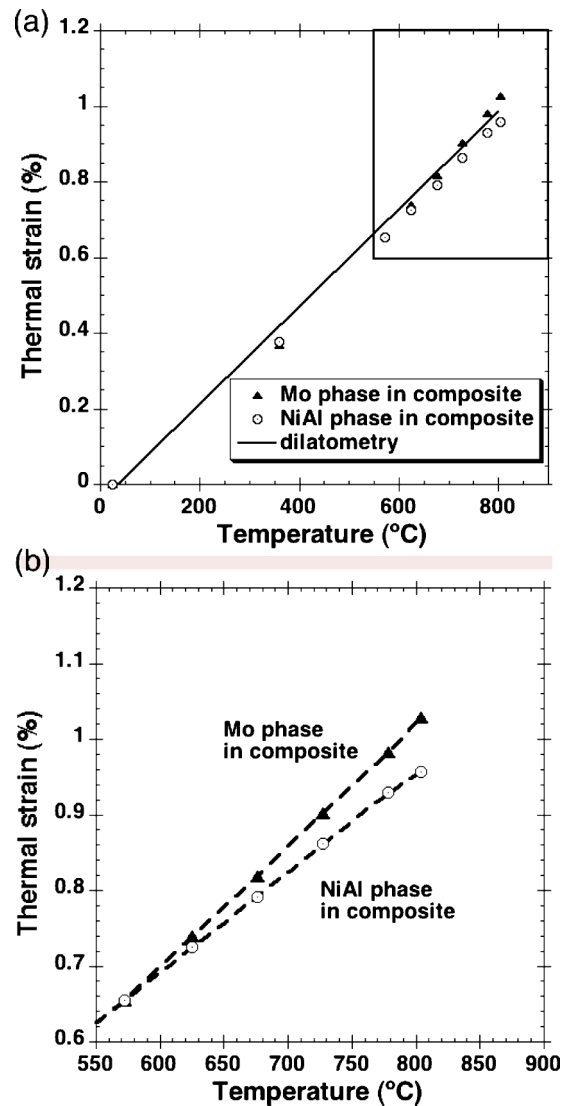


FIG. 3. (a) Temperature dependence of the {200}-specific thermal elastic strain in the NiAl and Mo_{ss} phases of the composite in the axial direction (i.e., parallel to the fibers). For comparison, the thermal strain of the composite measured by dilatometry is also shown. (b) Magnified portion of right upper corner of (a) showing that the Mo_{ss} phase expands more than the NiAl phase between 650 and 800 $^\circ\text{C}$.

posite. The two phases coexpand up to 650 $^\circ\text{C}$ with an average CTE of $12.8 \times 10^{-6} \text{ }^\circ\text{C}^{-1}$. For comparison, the composite CTE was determined by dilatometry measurements as the temperature was raised from room temperature to 800 $^\circ\text{C}$, and the results are shown as the straight line in Fig. 3(a). The average CTE obtained from the dilatometry measurements is $13.0 \times 10^{-6} \text{ }^\circ\text{C}^{-1}$, in agreement with the average CTE obtained from lattice-parameter (neutron-diffraction) measurements.

Beyond 650 $^\circ\text{C}$, the NiAl phase continues to expand with roughly the same slope as before [Fig. 3(b)]. However, the expansion of the Mo_{ss} phase increases abruptly, which is surprising because it has an intrinsically lower CTE than does NiAl (Fig. 2). This unexpected behavior appears to be related to the softening of the NiAl phase as the temperature increases and will be discussed later in terms of the mechanical loading results to be presented in the following section.

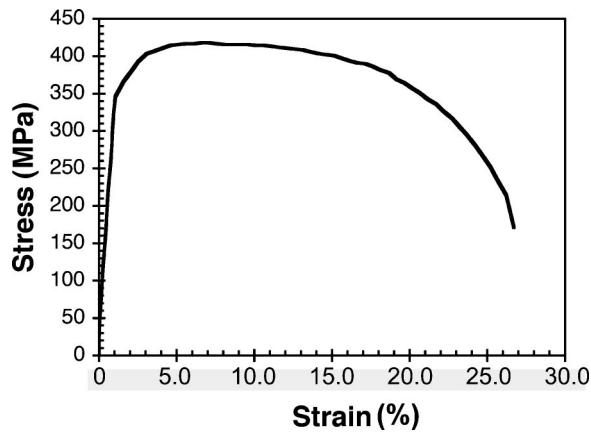


FIG. 4. Tensile stress-strain curve of the NiAl-Mo composite at 800 °C.

Response of the NiAl-Mo composite to mechanical loading

In situ neutron diffraction was conducted during tensile testing at 800 °C, which is above the ductile-to-brittle transition temperature (~ 650 °C) of the NiAl-Mo composite.¹⁰ Figure 4 shows the stress-strain curve of the composite recorded with a load cell and an extensometer spanning the gage length of the specimen during the *in situ* neutron diffraction. Initially, the composite responds in a linear elastic manner with a Young's modulus of ~ 30 GPa (determined from the slope of the elastic stress-strain curve). As will be discussed shortly, this low value for the modulus is due to extensive softening and plastic flow in the NiAl, which results in all the elastic strain being borne by the Mo fibers. The 0.2% offset yield stress is 331 MPa, beyond which the material work hardens slightly for the first few percent strain, and then softens before finally fracturing at $\sim 26\%$ strain.

Figure 5 shows the phase-specific $\{002\}$ elastic strain response of the NiAl and Mo_{ss} phases as a function of applied tensile stress in the axial and transverse directions. It is important to note that neutron diffraction measures only lattice-parameter changes and thus measures only the elastic

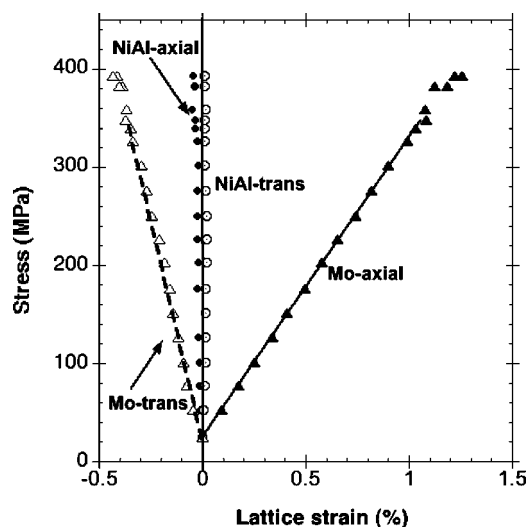


FIG. 5. Stress vs phase-specific lattice strain curves at 800 °C showing that elastic strains are produced only in the Mo_{ss} phase. The NiAl phase flows freely at this temperature and transfers all the load to the Mo_{ss} fibers.

strains in the individual phases. The lack of elastic strain development in the NiAl matrix in both the axial and transverse directions at 800 °C indicates that it flows freely in response to the applied load. At this temperature, the Mo_{ss} phase supports essentially the entire applied load. The slope of the Mo_{ss} stress-strain curve in the elastic region, when normalized to the effective area of the minority phase in the composite (14.1%), indicates a modulus of 214 GPa for the fibers. Additionally, the slope of the transverse stress-strain curve indicates a Poisson's ratio of 0.38.

DISCUSSION

The "coexpansion" of the composite constituents parallel to the fiber direction during heating to 650 °C is due to the constraint imposed on the fibers by the matrix and has been observed previously in both thermal¹⁷ and mechanical²⁰ loading of continuous fiber composites. Based on the measurements of phase-specific coefficients of thermal expansion, it is possible to estimate the thermal-expansion behavior of the overall composite. A simple rule of mixtures predicts that the thermal strain in the composite is given by

$$\varepsilon_c = \varepsilon_m V_m + \varepsilon_f V_f, \quad (3)$$

where $V_m = 0.859$ and $V_f = 0.141$ are the matrix and fiber volume fractions and ε_m and ε_f are the phase-specific thermal strains in the matrix and in the fibers, respectively. Each term on the left- and right-hand sides of Eq. (3) can be divided by the temperature difference over which the thermal strains are measured to obtain an analogous expression for CTEs, from which the CTE of the composite was determined to be 14.6×10^{-6} °C⁻¹. This value is similar to the composite CTE measured by dilatometry which, although varying with temperature, has an average value of $\sim 13.0 \times 10^{-6}$ °C⁻¹ from room temperature to 800 °C.

The deviation from codeformation behavior at 650 °C suggests that the NiAl matrix flows readily above this temperature. It is reasonable to associate this with the ductile-to-brittle transition reported in Ref. 10. Indeed, as the stress-strain curve shown in Fig. 5 demonstrates, at 800 °C, the NiAl matrix is unable to support any load whatsoever. Thus, the apparent increased rate of expansion of the Mo_{ss} above 650 °C is likely due to the softening of the NiAl. As discussed in the experimental section, the samples were held in place during the CTE measurement by a constant 20-MPa tensile load. Once the NiAl softens, this load is transferred entirely to the Mo_{ss} fibers, which constitute only about 14% of the volume of the composite. Indeed, the *in situ* loading data indicate that an applied stress of 20 MPa produces an additional elastic strain in the Mo_{ss} fibers of $\sim 660 \times 10^{-6}$ at 800 °C (Fig. 5), which corresponds well to the additional strain accumulated in the Mo_{ss} fibers when heated from 650 to 800 °C [Fig. 3(b)].

Our results provide further understanding of the thermo-mechanical behavior of long-fiber-reinforced metallic composites: e.g., in the transverse direction, the fibers and matrix expand independently, which appears to be a common characteristic of a continuous fiber-reinforced composite.¹⁷ Additionally, the mismatch in the phase-specific CTEs indicates

that thermal residual stresses can be generated in the composite, which may explain why interface debonding has been observed between the NiAl and Mo phases.¹⁰

CONCLUSIONS

Composites consisting of nanoscale Mo_{ss} fibers embedded in a NiAl matrix were produced by directional solidification, and their response to thermal and mechanical loading was studied. In the transverse direction (perpendicular to the fiber direction), the NiAl and Mo_{ss} phases expand independently and have average coefficients of thermal expansion of $16.0 \times 10^{-6} \text{ }^\circ\text{C}^{-1}$ and $5.8 \times 10^{-6} \text{ }^\circ\text{C}^{-1}$, respectively. In the axial direction (parallel to the fiber direction), the two phases coexpand up to 650 °C. Over this temperature range the lattice CTE of both constituents (measured by neutron diffraction) is $12.8 \times 10^{-6} \text{ }^\circ\text{C}^{-1}$, in agreement with the average CTE obtained by dilatometry measurements on the same composite. Between 650 and 800 °C, the Mo_{ss} phase expands more than the NiAl phase. This anomalous behavior appears to be related to the complete load transfer to the Mo_{ss} fibers after the NiAl matrix softens and cannot support any load.

ACKNOWLEDGMENTS

This research was sponsored by the Division of Materials Sciences and Engineering, Office of Basic Energy Sciences, U. S. Department of Energy under Contract No. DE-AC05-00OR22725 with UT-Battelle, LLC. This work also benefited from the use of the Los Alamos Neutron Science Center (LANSCE) at the Los Alamos National Laboratory funded by the US Department of Energy under Contract No. W-7405-ENG-36. The authors would like to thank T. Sis-

neros and Dr. B. Clausen at Los Alamos National Laboratory for their help and discussion in neutron-diffraction measurements.

- ¹S. V. Raj, I. E. Locci, J. A. Salem, and R. J. Pawlik, *Metall. Mater. Trans. A* **33**, 597 (2002).
- ²D. R. Johnson, X. F. Chen, B. F. Oliver, R. D. Noebe, and J. D. Whittenberger, *Intermetallics* **3**, 99 (1995).
- ³R. D. Noebe, A. Misra, and R. Gibala, *ISIJ Int.* **31**, 1172 (1991).
- ⁴H. E. Cline, J. L. Walter, E. Lifshin, and R. R. Russell, *Metall. Trans.* **2**, 189 (1971).
- ⁵H. Bei, G. M. Pharr, and E. P. George, *J. Mater. Sci.* **39**, 3975 (2004).
- ⁶A. Misra, Z. L. Wu, M. T. Kush, and R. Gibala, *Philos. Mag. A* **78**, 533 (1998).
- ⁷J. L. Walter and H. E. Cline, *Metall. Trans.* **4**, 33 (1973).
- ⁸P. R. Subramanian, M. G. Mendiratta, and D. B. Miracle, *Metall. Mater. Trans. A* **25**, 2769 (1994).
- ⁹A. Misra and R. Gibala, *Intermetallics* **8**, 1025 (2000).
- ¹⁰H. Bei and E. P. George, *Acta Mater.* **53**, 69 (2005).
- ¹¹M. Taya and R. J. Arsenault, *Metal Matrix Composites: Thermomechanical Behavior* (Pergamon, New York, 1989).
- ¹²R. S. Krishnan, R. Srinivasan, and S. Devanarayanan, *Thermal Expansion of Crystals* (Pergamon, New York, 1979).
- ¹³J. C. Hanan, E. Ustundag, B. Clausen, M. Sivasambu, I. J. Beyerlein, D. W. Brown, and M. A. M. Bourke, *Mater. Sci. Forum* **404-4**, 907 (2002).
- ¹⁴P. Rangaswamy, M. B. Prime, M. Daymond, M. A. M. Bourke, B. Clausen, H. Choo, and N. Jayaraman, *Mater. Sci. Eng., A* **259**, 209 (1999).
- ¹⁵M. A. M. Bourke, D. C. Dunand, and E. Ustundag, *Appl. Phys. A* **74**, s1707 (2002).
- ¹⁶R. B. Von Dreele, *J. Appl. Crystallogr.* **30**, 517 (1997).
- ¹⁷H. Choo, P. Rangaswamy, M. A. M. Bourke, and J. M. Larsen, *Mater. Sci. Eng., A* **325**, 236 (2002).
- ¹⁸R. W. Clark and J. D. Whittenberger, *Thermal Expansion*, edited by T. A. Hahn, (Plenum, New York, 1984), Vol. 8, p. 189.
- ¹⁹*Binary Alloy Phase Diagram*, edited by T. B. Massalski (American Society for Metals, Metals Park, OH, 1987).
- ²⁰P. J. Withers and A. P. Clarke, *Acta Mater.* **46**, 6585 (1998).